

Multiple Pathways for Benzyl Alcohol Oxidation by $\text{Ru}^{\text{V}}=\text{O}^{3+}$ and $\text{Ru}^{\text{IV}}=\text{O}^{2+}$

Amit Paul, Jonathan F. Hull, Michael R. Norris, Zuofeng Chen, Daniel H. Ess, Javier J. Concepcion, and Thomas J. Meyer*

Department of Chemistry, University of North Carolina at Chapel Hill, Chapel Hill, North Carolina 27599, United States

Received December 13, 2010

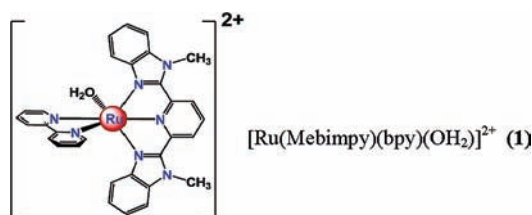
Significant rate enhancements are found for benzyl alcohol oxidation by the $\text{Ru}^{\text{V}}=\text{O}^{3+}$ form of the water oxidation catalyst $[\text{Ru}(\text{Mebimpy})(\text{bpy})(\text{OH}_2)]^{2+}$ [Mebimpy = 2,6-bis(1-methylbenzimidazol-2-yl)pyridine; bpy = 2,2'-bipyridine] compared to $\text{Ru}^{\text{IV}}=\text{O}^{2+}$ and for the $\text{Ru}^{\text{IV}}=\text{O}^{2+}$ form with added bases due to a new pathway, concerted hydride proton transfer (HPT).

There is an extensive literature of catalytic and mechanistic studies on alcohol oxidation by high-oxidation-state polypyridyl $\text{Ru}=\text{O}$.^{1–8} Multiple mechanisms have been proposed for these reactions including H-atom transfer,^{2,3,9} C–H insertion,^{10,11} and $2e^-/1\text{H}^+$ hydride transfer.^{3,12} Oxidants used in previous studies such as $[\text{Ru}^{\text{IV}}(\text{bpy})_2(\text{py})(\text{O})]^{2+}$ and $[\text{Ru}^{\text{IV}}(\text{tpy})(\text{bpy})(\text{O})]^{2+}$ (tpy = 2,2':6',2''-terpyridine) were kinetically slow and were limited to acidic solutions because of the instability of their high-oxidation-state forms toward ligand oxidation.^{4,5}

In a recent development, a related family of single-site water oxidation catalysts has been identified that functions both in solution and as phosphonate derivatives on electrode surfaces.^{13–17} An example is $[\text{Ru}(\text{Mebimpy})(\text{bpy})(\text{H}_2\text{O})]^{2+}$ (**1**). It undergoes oxidative activation by stepwise proton-coupled electron transfer (PCET), $\text{Ru}^{\text{II}}-\text{OH}_2^{2+} \xrightarrow{-e^-/-\text{H}^+} \text{Ru}^{\text{III}}-\text{OH}^{2+} \xrightarrow{-e^-/-\text{H}^+} \text{Ru}^{\text{IV}}=\text{O}^{2+}$,

followed by $1e^-$ oxidation to $\text{Ru}^{\text{V}}=\text{O}^{3+}$. With a family of oxidation catalysts available having properties systematically tunable by ligand variations, it is possible to decrease water oxidation as a background reaction and investigate oxidation of competing substrates based on both $\text{Ru}^{\text{IV}}=\text{O}^{2+}$ and the more powerful oxidant, $\text{Ru}^{\text{V}}=\text{O}^{3+}$.

We report here the results of a preliminary study on the oxidation of benzyl alcohol (BnOH) by the $\text{Ru}^{\text{IV}}=\text{O}^{2+}$ and $\text{Ru}^{\text{V}}=\text{O}^{3+}$ forms of (**1**). The results are notable in demonstrating a significant rate enhancement for $\text{Ru}^{\text{V}}=\text{O}^{3+}$ compared to $\text{Ru}^{\text{IV}}=\text{O}^{2+}$ and in identifying multiple pathways for alcohol oxidation by $\text{Ru}^{\text{IV}}=\text{O}^{2+}$ including a novel base-assisted pathway that appears to involve concerted hydride proton transfer (HPT).¹⁸



Synthesis and characterization of the catalyst were reported elsewhere.^{19,20} At pH = 1, $E_{1/2}$ values for the pH-dependent $\text{Ru}^{\text{III}}-\text{OH}_2^{3+}/\text{Ru}^{\text{II}}-\text{OH}_2^{2+}$ and $\text{Ru}^{\text{IV}}=\text{O}^{2+}/\text{Ru}^{\text{III}}-\text{OH}_2^{3+}$ couples are 0.82 and 1.30 V versus normal hydrogen electrode (NHE). For the pH-independent $\text{Ru}^{\text{V}}=\text{O}^{3+}/\text{Ru}^{\text{IV}}=\text{O}^{2+}$ couple, $E_{1/2} = 1.65$ V.¹⁹ For convenience, a plot of $E_{1/2}$ versus pH and a listing of $E_{1/2}$ values are given in Supporting Information, Figure SI 1 and Table SI 1.

For kinetic measurements, cyclic voltammetry experiments were performed at a boron-doped diamond (BDD) electrode. In Figure 1 is shown a series of cyclic voltammograms of (**1**) at pH = 7.4 in a phosphate buffer ($\text{H}_2\text{PO}_4^-/\text{HPO}_4^{2-}$) in KNO_3 ($I = 0.1$ M) with increasing concentrations of added BnOH. Under these conditions, the peak-to-peak separation for the $\text{Ru}^{\text{IV}}=\text{O}^{2+}/\text{Ru}^{\text{III}}-\text{OH}_2^{3+}$ couple at $E_{1/2} = 0.95$ V is much greater than 60 mV and wave forms are broadened because of kinetically slow PCET oxidation of $\text{Ru}^{\text{III}}-\text{OH}_2^{3+}$ to $\text{Ru}^{\text{IV}}=\text{O}^{2+}$.²¹

(18) Ess, D. H.; Schauer, C. K.; Meyer, T. J. *J. Am. Chem. Soc.* **2010**, *132*, 16318.

(19) Concepcion, J. J.; Jurss, J. W.; Norris, M. R.; Chen, Z.; Templeton, J. L.; Meyer, T. J. *Inorg. Chem.* **2010**, *49*, 1277.

(20) Concepcion, J. J.; Tsai, M.-K.; Muckerman, J. T.; Meyer, T. J. *J. Am. Chem. Soc.* **2010**, *132*, 1545.

(21) Trammell, S. A.; Wimbish, J. C.; Odobel, F.; Gallagher, L. A.; Narula, P. M.; Meyer, T. J. *J. Am. Chem. Soc.* **1998**, *120*, 13248.

*To whom correspondence should be addressed. E-mail: tjmeyer@unc.edu.

(1) Bryant, J. R.; Matsuo, T.; Mayer, J. M. *Inorg. Chem.* **2004**, *43*, 1587.

(2) Matsuo, T.; Mayer, J. M. *Inorg. Chem.* **2005**, *44*, 2150.

(3) Meyer, T. J.; Huynh, M. H. V. *Inorg. Chem.* **2003**, *42*, 8140.

(4) Roecker, L.; Meyer, T. J. *J. Am. Chem. Soc.* **1987**, *109*, 746–754.

(5) Thompson, M. S.; Meyer, T. J. *J. Am. Chem. Soc.* **1982**, *104*, 4106.

(6) Thompson, M. S.; Meyer, T. J. *J. Am. Chem. Soc.* **1982**, *104*, 5070.

(7) Marmion, M. E.; Takeuchi, K. J. *J. Am. Chem. Soc.* **1988**, *110*, 1472.

(8) Muller, J. G.; Acquaye, J. H.; Takeuchi, K. J. *Inorg. Chem.* **1992**, *31*, 4552.

(9) Seok, W. K.; Meyer, T. J. *Inorg. Chem.* **2005**, *44*, 3931–3941.

(10) Gallagher, L. A.; Meyer, T. J. *J. Am. Chem. Soc.* **2001**, *123*, 5308.

(11) Stultz, L. K.; Huynh, M. H. V.; Binstead, R. A.; Curry, M.; Meyer, T. J. *J. Am. Chem. Soc.* **2000**, *122*, 5984.

(12) Dolega, A. *Coord. Chem. Rev.* **2010**, *254*, 916.

(13) Chen, Z.; Concepcion, J. J.; Hu, X.; Yang, W.; Hoertz, P. G.; Meyer, T. J. *Proc. Natl. Acad. Sci. U.S.A.* **2010**, *107*, 7225.

(14) Chen, Z.; Concepcion, J. J.; Hull, J. F.; Hoertz, P. G.; Meyer, T. J. *Dalton Trans.* **2010**, *39*, 6950.

(15) Chen, Z.; Concepcion, J. J.; Jurss, J. W.; Meyer, T. J. *J. Am. Chem. Soc.* **2009**, *131*, 15580–15581.

(16) Chen, Z.; Concepcion, J. J.; Luo, H.; Hull, J. F.; Paul, A.; Meyer, T. J. *J. Am. Chem. Soc.* **2010**, *132*, 17670.

(17) Concepcion, J. J.; Jurss, J. W.; Brennaman, M. K.; Hoertz, P. G.; Patrocino, A. O. v. T.; Murakami Iha, N. Y.; Templeton, J. L.; Meyer, T. J. *Acc. Chem. Res.* **2009**, *42*, 1954.

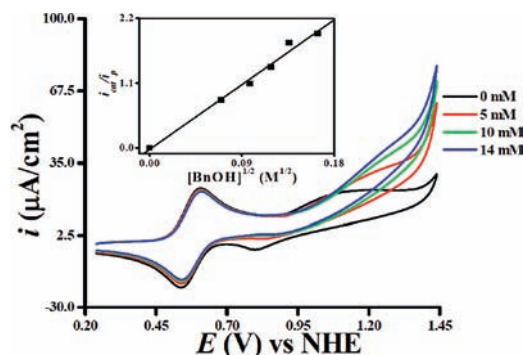


Figure 1. Cyclic voltammograms (vs NHE) of 1 mM (I) in a 30 mM phosphate buffer ($\text{H}_2\text{PO}_4^-/\text{HPO}_4^{2-}$) at pH = 7.4 ($I = 0.1$ M; KNO_3 , 21 ± 2 °C) at 10 mV s^{-1} , showing the influence of added BnOH on the oxidative wave for the $\text{Ru}^{\text{IV}}=\text{O}^{2+}/\text{Ru}^{\text{III}}\text{-OH}^{2+}$ couple at $E_{1/2} = 0.95$ V at this pH (Figure SI (I) in the Supporting Information). The electrode was BDD (0.07 cm^2). In the inset is shown a plot of $i_{\text{cat}}/i_{\text{p}}$ at 1.24 V vs $[\text{BnOH}]^{1/2}$, see the text.

At a scan rate of 10 mV s^{-1} , $E_{\text{p,a}}$ for the $\text{Ru}^{\text{IV}}=\text{O}^{2+}/\text{Ru}^{\text{III}}\text{-OH}^{2+}$ couple appears at ~ 1.24 V with and without added BnOH. As shown in the inset in Figure 1, with added BnOH, the current ratio ($i_{\text{cat}}/i_{\text{p}}$) at 1.24 V increases linearly with $[\text{BnOH}]^{1/2}$ (i_{p} and i_{cat} are the peak currents without and with added alcohol). This potential was chosen for analysis because it is the peak potential for the oxidative component of the $\text{Ru}^{\text{IV}}=\text{O}^{2+}/\text{Ru}^{\text{III}}\text{-OH}^{2+}$ wave and it is well separated from the $\text{Ru}^{\text{V}}=\text{O}^{3+}/\text{Ru}^{\text{IV}}=\text{O}^{2+}$ couple at $E_{1/2} = 1.65$ V. The latter dominates catalysis at higher potentials; see below. The ratio $i_{\text{cat}}/i_{\text{p}}$ varies linearly with $1/\nu^{1/2}$ (ν is the scan rate) over the range $10\text{--}200 \text{ mV s}^{-1}$. i_{cat} increases linearly with a change in the complex concentration from 0.13 to 1.0 mM.

Catalytic rate constants, k_{cat} , were determined from the peak current ratio by use of eq 1.²² In eq 1, R , T , n , F , and ν are the gas constant, temperature, number of electrons transferred ($n = 2$ for BnOH oxidation to benzaldehyde; see below), Faraday constant, and scan rate, respectively. Current measurements under argon and in air gave the same results in this and other studies reported here.

$$\frac{i_{\text{cat}}}{i_{\text{p}}} = \frac{(RT)^{1/2}}{0.446(nF\nu)^{1/2}} k_{\text{cat}}^{1/2} = \frac{(RT)^{1/2}}{0.446(nF\nu)^{1/2}} k^{1/2} (\text{BnOH})^{1/2} \quad (1)$$

The scan rate and concentration dependences of $i_{\text{cat}}/i_{\text{p}}$ are consistent with eq 1 with $k_{\text{cat}} = k_{\text{Ru}^{\text{IV}}}\text{[BnOH]}$ and the rate law in eq 2a. Kinetic measurements were also performed in 0.1 M KNO_3 (pH = 7) at 21 ± 2 °C and at pH = 2.5 and 3.0 with added HNO_3 with no evidence for a pH dependence over the pH range 2.5–7. The average rate constant from the three sets of measurements gave $k_{\text{Ru}^{\text{IV}}} = 16 \pm 1 \text{ M}^{-1} \text{ s}^{-1}$. For comparison, $k_{\text{Ru}^{\text{IV}}} = 2.43 \pm 0.03 \text{ M}^{-1} \text{ s}^{-1}$ for oxidation of BnOH by *cis*- $[\text{Ru}^{\text{IV}}(\text{bpy})_2(\text{py})(\text{O})]^{2+}$ under similar conditions.⁴

$$\text{rate} = k_{\text{cat}}[\text{Ru}^{\text{IV}}=\text{O}^{2+}] = k_{\text{Ru}^{\text{IV}}}[\text{Ru}^{\text{IV}}=\text{O}^{2+}][\text{BnOH}] \quad (2a)$$

$$\text{rate} = k_{\text{cat}}[\text{Ru}^{\text{V}}=\text{O}^{3+}] = k_{\text{Ru}^{\text{V}}}[\text{Ru}^{\text{V}}=\text{O}^{3+}][\text{BnOH}] \quad (2b)$$

In order to verify benzaldehyde as a major product, a controlled potential electrolysis experiment was conducted.

Table 1. Rate Constants for BnOH Oxidation by $\text{Ru}^{\text{IV}}=\text{O}^{2+}$ and $\text{Ru}^{\text{V}}=\text{O}^{3+}$ at 21 ± 2 °C, $I = 0.1$ M (KNO_3)

base (B)	$\text{p}K_{\text{a}}$ (HB)	$k_{\text{B}} \times 10^{-2} (\text{M}^{-2} \text{ s}^{-1})$
OAc^-	4.7	2.4 ± 0.9
HPO_4^{2-}	7.2	5.8 ± 0.4
PO_4^{3-}	12.3	77 ± 9
$k_{\text{Ru}^{\text{IV}}}$		$16 \pm 1 \text{ M}^{-1} \text{ s}^{-1}$
$k_{\text{Ru}^{\text{V}}}$		$3230 \pm 50 \text{ M}^{-1} \text{ s}^{-1}$

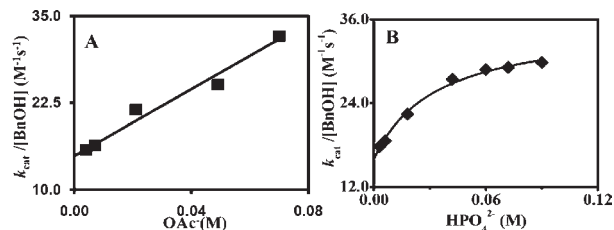


Figure 2. Plots of $k_{\text{cat}}/[\text{BnOH}]$ vs $[\text{OAc}^-]$ at pH = 5.1 (A) and vs $[\text{HPO}_4^{2-}]$ at pH = 7.4 (B) for oxidation of BnOH by $\text{Ru}^{\text{IV}}=\text{O}^{2+}$ at 21 ± 2 °C with $I = 0.1$ M (KNO_3).

In this experiment, $[\text{BnOH}] = 97 \text{ mM}$ and $[\text{Ru-OH}_2]^{2+} = 2 \text{ mM}$ with electrolysis at a *nano*-indium–tin oxide electrode²³ ($\sim 5 \mu\text{m}$, 0.72 cm^2) at 1.34 V vs NHE in a pH = 7.4 $\text{H}_2\text{PO}_4^-/\text{HPO}_4^{2-}$ buffer ($I = 0.1$ M). Electrolysis was continued for 580 min with stirring, with a steady-state current density of $140 \mu\text{A cm}^{-2}$ reached after 2000 s. Following extraction by chloroform, $^1\text{H NMR}$ showed the presence of benzaldehyde (95%) and a small amount of benzoic acid (5%) in the chloroform layer. The total faradaic efficiency was 76%.

In 0.1 M HNO_3 , greatly enhanced catalytic currents were observed when oxidative scans were extended to the $\text{Ru}^{\text{V}}=\text{O}^{3+}/\text{Ru}^{\text{IV}}=\text{O}^{2+}$ wave at $E_{1/2} = 1.65$ V. $i_{\text{cat}}/i_{\text{p}}$, measured at $E_{\text{p,a}} = 1.74$ V for this couple, varied with $[\text{BnOH}]^{1/2}$ over the range $0.1\text{--}0.6$ mM. Analysis of the data with the rate law in eq 2b gave $k_{\text{Ru}^{\text{V}}} = (3.2 \pm 0.1) \times 10^3 \text{ M}^{-1} \text{ s}^{-1}$ (Table 1). A comparison of the rate constant data in Table 1 shows a rate enhancement of ~ 200 for BnOH oxidation by $\text{Ru}^{\text{V}}=\text{O}^{3+}$ compared to $\text{Ru}^{\text{IV}}=\text{O}^{2+}$. With isopropyl alcohol as the added alcohol, $k_{\text{Ru}^{\text{V}}} = 320 \pm 20 \text{ M}^{-1} \text{ s}^{-1}$.

Oxidation of BnOH by $\text{Ru}^{\text{IV}}=\text{O}^{2+}$ below pH = 2.5 could not be studied because of the greatly enhanced reactivity of $\text{Ru}^{\text{V}}=\text{O}^{3+}$ due to the closely spaced $E_{1/2}$ values for the $\text{Ru}^{\text{V}}=\text{O}^{3+}/\text{Ru}^{\text{IV}}=\text{O}^{2+}$ and $\text{Ru}^{\text{IV}}=\text{O}^{2+}/\text{Ru}^{\text{III}}\text{-OH}^{2+}$ couples (Figure SI 1). Studies of BnOH oxidation by $\text{Ru}^{\text{V}}=\text{O}^{3+}$ were restricted to pH = 1 because of competitive water oxidation at higher pHs.¹³

Oxidation of BnOH by $\text{Ru}^{\text{IV}}=\text{O}^{2+}$ is buffer-base-dependent. In Figure 2 are shown plots of $k_{\text{cat}}/[\text{BnOH}]$ at fixed pH (5.1 for acetic acid/acetate HOAc/OAc^- ; 7.4 for $\text{H}_2\text{PO}_4^-/\text{HPO}_4^{2-}$) for the added buffer bases OAc^- and HPO_4^{2-} . As shown in Figure 2A, $k_{\text{cat}}/[\text{BnOH}]$ increased linearly with $[\text{OAc}^-]$. Extrapolation to $[\text{OAc}^-] = 0$ gave $k = 15 \text{ M}^{-1} \text{ s}^{-1}$, consistent with $k_{\text{Ru}^{\text{IV}}} = 16 \text{ M}^{-1} \text{ s}^{-1}$ in the absence of added buffer. These observations are consistent with the rate law in eq 3 and an additional term for BnOH oxidation first order in $[\text{OAc}^-]$. From the slope of the plot in Figure 2A, $k_{\text{B}} = k_{\text{OAc}^-} = 240 \pm 94 \text{ M}^{-2} \text{ s}^{-1}$ (Table 1).

$$\text{rate} = k_{\text{cat}}[\text{Ru}^{\text{IV}}=\text{O}^{2+}] = \{k_{\text{Ru}^{\text{IV}}} + k_{\text{OAc}^-}[\text{OAc}^-]\}[\text{Ru}^{\text{IV}}=\text{O}^{2+}][\text{BnOH}] \quad (3)$$

With added HPO_4^{2-} , there is evidence for saturation kinetics at high $[\text{HPO}_4^{2-}]$ (Figure 2B and the mechanism in eq 4 with preliminary ion-pair formation, eq 4a, followed by

(22) Galus, Z. *Fundamentals of Electrochemical Analysis*; Ellis Horwood Ltd.: Chichester, U.K., 1976.

(23) Hoertz, P. G.; Chen, Z.; Kent, C. A.; Meyer, T. J. *Inorg. Chem.* **2010**, *49*, 8179.

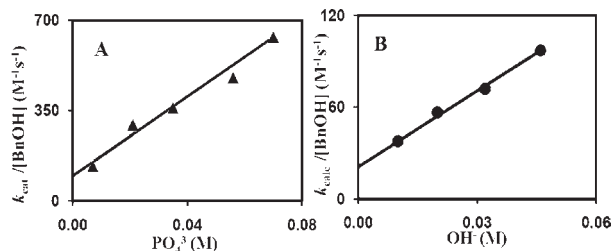
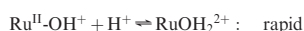
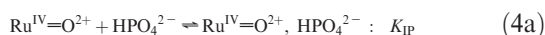


Figure 3. (A) Plot of $k_{\text{cat}}/[\text{BnOH}]$ vs $[\text{PO}_4^{3-}]$ at $\text{pH} = 12.7$ and (B) plot of $k_{\text{cat}}/[\text{BnOH}]$ vs $[\text{OH}^-]$ for BnOH oxidation by $\text{Ru}^{\text{IV}}=\text{O}^{2+}$ over the pH range 12–12.7 at $21 \pm 2^\circ\text{C}$ with $I = 0.1\text{ M}$ (KNO_3); see the text.

oxidation, eq 4b). The rate law is given in eq 5. The experimental points in Figure 2B were fit to the rate law in eq 5 with $k_{\text{Ru}^{\text{IV}}} = 16\text{ M}^{-1}\text{ s}^{-1}$, $K_{\text{IP}} = 30\text{ M}^{-1}$, $k_{\text{red}} = 20\text{ M}^{-1}\text{ s}^{-1}$, and $k_{\text{HPO}_4^{2-}} = k_{\text{red}}K_{\text{IP}} = 576 \pm 44\text{ M}^{-2}\text{ s}^{-1}$ (Table 1).



$$\text{rate} = \{k_{\text{Ru}^{\text{IV}}} + (K_{\text{IP}}k_{\text{red}}[\text{HPO}_4^{2-}]) / (1 + K_{\text{IP}}[\text{HPO}_4^{2-}])\} [\text{Ru}^{\text{IV}}=\text{O}^{2+}] [\text{BnOH}] \quad (5a)$$

$$k_{\text{cat}} = \{k_{\text{Ru}^{\text{IV}}} + (K_{\text{IP}}k_{\text{red}}[\text{HPO}_4^{2-}]) / (1 + K_{\text{IP}}[\text{HPO}_4^{2-}])\} [\text{BnOH}] \quad (5b)$$

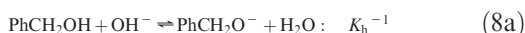
An additional rate enhancement was observed at $\text{pH} = 12.7$ with added $\text{HPO}_4^{2-}/\text{PO}_4^{3-}$ buffer. As shown in Figure 3A, $k_{\text{cat}}/[\text{BnOH}]$ increased linearly with $[\text{PO}_4^{3-}]$, consistent with the rate law in eq 6 and a term first order in PO_4^{3-} . From the slope of the plot, $k_{\text{PO}_4^{3-}} = 7700 \pm 900\text{ M}^{-2}\text{ s}^{-1}$ (Table 1).

$$\text{rate} = \{k_0 + k_{\text{HPO}_4^{2-}}[\text{HPO}_4^{2-}] + k_{\text{PO}_4^{3-}}[\text{PO}_4^{3-}]\} [\text{Ru}^{\text{IV}}=\text{O}^{2+}] [\text{BnOH}] \quad (6)$$

$$\text{rate} = \{k_{\text{Ru}^{\text{IV}}} + k_{\text{OH}^-}[\text{OH}^-] + k_{\text{HPO}_4^{2-}}[\text{HPO}_4^{2-}] + k_{\text{PO}_4^{3-}}[\text{PO}_4^{3-}]\} [\text{Ru}^{\text{IV}}=\text{O}^{2+}] [\text{BnOH}] \quad (7)$$

The intercept of the plot in Figure 3A is $97\text{ M}^{-1}\text{ s}^{-1}$, considerably higher than the value $k_{\text{Ru}^{\text{IV}}} = 16\text{ M}^{-1}\text{ s}^{-1}$. This suggested a possible role for OH^- as a proton acceptor base. To explore this possibility, experiments were conducted in the pH range 12–12.7 by varying the $[\text{HPO}_4^{2-}]/[\text{PO}_4^{3-}]$ ratio with 10 mM total added buffer ($I = 0.1\text{ M}$). k_{cat} values were obtained at zero buffer base concentration at each pH by subtracting contributions from the PO_4^{3-} pathway from k_{cat} values obtained experimentally by using eq 6 and the known value of $k_{\text{PO}_4^{3-}}$. Under these conditions, the $k_{\text{HPO}_4^{2-}}[\text{HPO}_4^{2-}]$ term was negligible. As shown in Figure 3B, $k_{\text{cat}}/[\text{BnOH}]$ increases linearly with $[\text{OH}^-]$ over the pH range 12–12.7, consistent with an additional pathway first order in $[\text{OH}^-]$. The complete rate law is given in eq 7. From the slope of the plot in Figure 3B, $k_{\text{OH}^-} = 1650 \pm 540\text{ M}^{-2}\text{ s}^{-1}$ (Table 1).

A reasonable interpretation for the OH^- pathway is that initial proton loss occurs followed by rapid oxidation of the anion, BnO^- (eq 8). The rate law for this mechanism is given in eq 9 with K_{h} the hydrolysis constant for the equilibrium: $\text{PhCH}_2\text{O}^- + \text{H}_2\text{O} \rightleftharpoons \text{PhCH}_2\text{OH} + \text{OH}^-$ ($K_{\text{w}}/K_{\text{a}} = 0.1$) with $\text{p}K_{\text{a}} = 15$ for benzyl alcohol. With this interpretation, $k_{\text{BnO}^-} = 1.7 \times 10^4\text{ M}^{-2}\text{ s}^{-1}$.



$$\text{rate} = \{k_{\text{Ru}^{\text{IV}}} + k_{\text{BnO}^-}K_{\text{h}}^{-1}[\text{OH}^-]\} [\text{Ru}^{\text{IV}}=\text{O}^{2+}] [\text{PhCH}_2\text{OH}] \quad (9)$$

The results reported here are notable in expanding the known reactivity of $\text{Ru}=\text{O}$ complexes toward alcohol oxidation. Although detailed mechanistic studies, including supporting density functional theory calculations and C–H/C–D kinetic isotope effects, are currently under investigation, important features have already been revealed:

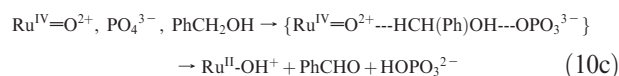
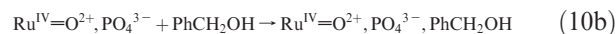
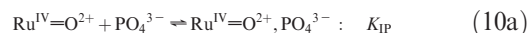
(i) $\text{Ru}^{\text{V}}=\text{O}^{3+}$, as $[\text{Ru}^{\text{V}}(\text{Mebimpy})(\text{bpy})(\text{O})]^{3+}$, is a facile oxidant, ~ 200 times more reactive than $\text{Ru}^{\text{IV}}=\text{O}^{2+}$ toward BnOH oxidation.

(ii) There is no O_2 dependence for BnOH oxidation by either $\text{Ru}^{\text{IV}}=\text{O}^{2+}$ or $\text{Ru}^{\text{V}}=\text{O}^{3+}$. This is in contrast to the $[\text{Ru}^{\text{IV}}(\text{bpy})_2(\text{py})(\text{O})]^{2+}$ oxidations of isopropyl alcohol and benzyl alcohol, both of which exhibit O_2 dependences.^{5,9} The absence of O_2 dependence is consistent with $2e^-$ pathways and net hydride transfer or C–H insertion, although the microscopic details remain to be elucidated.³

(iii) Deprotonation to PhCH_2O^- results in a rate enhancement of $\sim 10^3$ compared to PhCH_2OH by a mechanism that appears to involve hydride ($2e^-/1\text{H}^+$) transfer.¹⁸

(iv) The pathway first order in added base (OAc^- , HPO_4^{2-} , and PO_4^{3-}) is a new pathway that does not involve prior deprotonation and PhCH_2O^- oxidation because $k_{\text{B}} > k_{\text{BnO}^-}K_{\text{h}}^{-1}[\text{OH}^-]$ for all three bases.

The appearance of the new base-catalyzed pathway is notable. It points to a pathway for alcohol dehydrogenation by concerted HPT:¹⁸



This pathway avoids the protonated aldehyde PhCHOH^+ as a high-energy intermediate and is qualitatively consistent with the dependence of k_{B} on the strength of the acceptor base ($-RT \ln K_{\text{a}}$) in Table 1. It is different from typical concerted transfer hydrogenation mechanisms, such as those described by Knowles and Noyori,^{24–26} but is related to multicomponent or bifunctional hydrogenation mechanisms.²⁷

(i) The acceleration with PO_4^{3-} is especially notable, with a rate acceleration of ~ 40 in 0.1 M PO_4^{3-} compared to water, which may be of relevance in electrocatalysis.

Acknowledgment. Primary support for this research came from the CCHF, an EFRC funded by the U.S. DOE under Award DE-SC0001298 at the University of Virginia. Support also came from UNC EFRC, an EFRC funded by the U.S. DOE under Award DE-SC0001011 and is gratefully acknowledged.

Supporting Information Available: Additional supporting electrochemical results and discussion. This material is available free of charge via the Internet at <http://pubs.acs.org>.

(24) Knowles, W. S.; Noyori, R. *Acc. Chem. Res.* **2007**, *40*, 1238.

(25) Jessop, P. G.; Ikariya, T.; Noyori, R. *Chem. Rev.* **1995**, *95*, 259.

(26) Dobreiner, G. E.; Crabtree, R. H. *Chem. Rev.* **2010**, *110*, 681.

(27) Simoln, L.; Goodman, J. M. *J. Am. Chem. Soc.* **2008**, *130*, 8741.